20TH, GIFU ISTS & 11TH IAS

96-g-11

Hydrodynamic Instability Consideration for Material Processing in Space

M. Goto, A. Fridberg,
and P. D. Weidman
University of Colorado at Boulder

20th International Symposium
on Space Technology and Science
Gifu, Japan
May 19 - 25, 1996

20th ISTS Secretariat
Hamamatsu-cho Central Building, 1-29-6 Hamamatsu-cho
Minato-ku, Tokyo 105
JAPAN

HYDRODYNAMIC INSTABILITY CONSIDERATION FOR MATERIAL PROCESSING IN SPACE

Makoto Goto*, Anders Fridberg** and Patrick D. Weidman***

Dept. of Mechanical Engineering, Univ. of Colorado at Boulder

Abstract

In using the space environment for material processing, fundamental fluid mechanical problems intrinsic to the processing configuration should be identified and studied to improve the grade of the products further. The present investigation addresses the stability of a rotating column of two immiscible liquids of different density surrounded by an impermeable cylindrical boundary in the absence of gravity, and summarizes the effect of parameters deduced naturally in nondimensionalizing basic equations on hydrodynamic instability.

1. Introduction

Processing of special materials or medicines in space is more advantageous than conventional processing techniques because its low gravity field can yield improved purity and uniformity of the products. Currently, material processing in space is in a testing phase; however, with the advent of the space station, it is expected to be more proliferated in the future. In using the space environment for material processing, fundamental fluid mechanical problems intrinsic to the processing configuration should be identified and studied to improve the grade of the products further.

The present investigation addresses the stability of a rotating column of two immiscible liquids of different density surrounded by an impermeable cylindrical boundary in the absence of gravity. In any real application to material processing in space, the cylinder will be of finite length have various boundary conditions imposed on each end, and the fluid within will be viscous. As a first approximation, an inviscid two-fluid system contained in a cylinder of infinite length is considered so that variations along the axial coordinate can be ignored.

Here only linear stability theory is applied, so the effect of nonlinearity, imperfect bifurcation, *etc.*, are not considered. Stability results for single component rotating liquids with free surfaces in zero gravity are presently available. These include studies on rotating liquid columns with an outer free surface by Hocking and Michael[3] and Hocking[4], and studies by Yih[10] and Pedley[6] for rotating flow either exterior or interior to a cylindrical boundary. Boudourides and Davis[1] presented some generalized Rayleigh stability criteria for free surface rotating liquid systems with consideration given to both viscous and inviscid fluids.

In a general rotating liquid system with interfacial surface tension, one expects three types of instability to occur. There is Rayleigh instability in the bulk fluid brought about by centrifugal forces, capillary instability, and Rayleigh-Taylor instability. In the present investigation only rigid rotation at angular velocity Ω is considered. Hence there can be no axisymmetric centrifugal instability since in each fluid phase the Rayleigh discriminant[2]

$$\Phi(r) = \frac{1}{r^3}\frac{d}{dr}(r^2\Omega)^2 = 4\Omega^2$$

is positive. Consequently, instability may arise either through Rayleigh-Taylor instability or through the effect of surface tension at a liquid-liquid interface or at a free surface.

2. Equation of Motion

The configuration sketched in Figure 1 exhibits the cylindrical polar coordinate system (r, θ, z), the interfacial boundary at $r = a$, and the cylinder wall at $r = b$. The constant fluid densities and

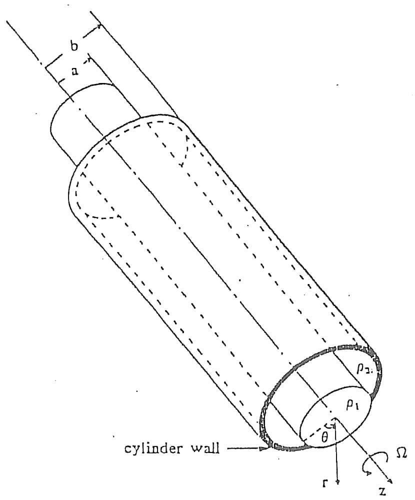

Figure 1 Schematic diagram of the rotating immiscible two-fluid system with interface at $r=a$ and outer cylinder at $r=b$. Also shown is the cylindrical (r, θ, z) coordinate system.

*Corresponding Author
Current Address: NISSAN Motor Co. Ltd., Aerospace Div.: 5-1, Momoi, 3-chome, Suginami-ku, Tokyo 167, Japan
Tel:(03)3301-6623; Fax:(03)3301-6718; e-mail: gotomak@nova.lab.nissan.co.jp
**Visitting Graduate Student
***Associate Professor

viscosties are ρ_i and μ_i, where subscripts 1 and 2 denote inner and outer fluids, respectively. The interfacial surface tension coefficient γ is also assumed constant. Motion of the fluid in each region is governed by the Navier-Stokes equations in a frame of reference rotating about the z-axis at angular velocity Ω and the equation of continuity in which t is the time variable, and $\mathbf{u}_i$, p_i, and ν_i are the velocity, pressure, and kinematic viscosity in each fluid region. The (r, θ, z) component velocities relative to the rotating frame are respectively (u_i, v_i, w_i). Scaling time with Ω^{-1}, lengths with the interfacial radius a, velocities with Ωa and pressures with $\rho_2\Omega^2a^2$, the nondimensional component form of equations in cylindrical coordinates are

$$\frac{\partial u_i}{\partial t} + (\mathbf{u}_i \bullet \nabla)u_i - \frac{v_i^2}{r} - 2v_i = -\frac{1}{\lambda^{2-i}}\frac{\partial}{\partial r}\left[p_i - \frac{\lambda^{2-i}}{2}r^2\right] + \frac{1}{R_i}\left[\Delta u_i - \frac{u_i}{r^2} - \frac{2}{r^2}\frac{\partial v_i}{\partial \theta}\right] \quad (2.1a)$$

$$\frac{\partial v_i}{\partial t} + (\mathbf{u}_i \bullet \nabla)v_i + \frac{u_i v_i}{r} + 2u_i = -\frac{1}{\lambda^{2-i}}\frac{1}{r}\frac{\partial p_i}{\partial \theta} + \frac{1}{R_i}\left[\Delta v_i - \frac{v_i}{r^2} + \frac{2}{r^2}\frac{\partial u_i}{\partial \theta_i}\right] \quad (2.1b)$$

$$\frac{\partial w_i}{\partial t} + (\mathbf{u}_i \bullet \nabla)w_i = -\frac{1}{\lambda^{2-i}}\frac{\partial p_i}{\partial z} + \frac{1}{R_i}\Delta w_i \quad (2.1c)$$

$$\frac{1}{r}\frac{\partial}{\partial r}(ru_i) + \frac{1}{r}\frac{\partial v_i}{\partial \theta} + \frac{\partial w_i}{\partial z} = 0, \quad (2.1d)$$

where $\lambda = \rho_1/\rho_2$ is the density ratio and $R_i = \Omega a^2/\nu_i$ are the interfacial Reynolds numbers of the inner (i=1) and outer (i=2) fluids. The undisturbed interface is conveniently positioned at $r = 1$ and the outer cylinder wall is located at $r = \kappa$, where $\kappa = b/a$ is the inverse radius ratio. Note that the limit $\kappa \to \infty$ is taken holding the interface radius constant, so that the two-fluid interface is always present in that limit. The position of the disturbed interface is denoted $r = 1 + \eta(\theta, z, t)$ and $\mathbf{n}$ is the local outward normal unit to the interface. Viscous boundary condition on the axis and at the impermeable outer wall are, respectively

$$p_1 = p_0, \ @r = 0 \quad (2.2a)$$

$$\mathbf{u}_2 = 0, \ @r = \kappa. \quad (2.2b)$$

The interfacial conditions are continuity of normal particle velocity

$$u_i = \frac{\partial \eta}{\partial t} + \frac{v_i}{r}\frac{\partial \eta}{\partial \theta} + w_i\frac{\partial \eta}{\partial z}, \ @r = 1 + \eta \quad (2.2c)$$

continuity of normal stress

$$p_2 - p_1 = \frac{2}{R_2}\left[\frac{\partial u_2}{\partial r} - \chi\frac{\partial u_1}{\partial r}\right] - L_2\nabla \bullet \mathbf{n}, \ @r = 1 + \eta \quad (2.2d)$$

and continuity of the tangential stresses

$$\chi\left[\frac{\partial v_1}{\partial r} - \frac{v_1}{r} + \frac{1}{r}\frac{\partial u_1}{\partial \theta}\right] = \left[\frac{\partial v_2}{\partial r} - \frac{v_2}{r} + \frac{1}{r}\frac{\partial u_2}{\partial \theta}\right], \ @r = 1 + \eta \quad (2.2e)$$

$$\chi\left[\frac{\partial u_1}{\partial z} + \frac{\partial w_1}{\partial r}\right] = \left[\frac{\partial u_2}{\partial z} + \frac{\partial w_2}{\partial r}\right], \ @r = 1 + \eta. \quad (2.2f)$$

where $\chi = \mu_1/\mu_2$ is the ratio of absolute viscosities and, generalizing the notation of Hocking[4] we define $L_i = \gamma/\rho_i\Omega^2a^3$ as the ratio of surface tension forces to centrifugal forces of fluid i = 1 or 2 at the interface.

Disturbance Equations

The base state in the rotating frame is one of zero velocity in each fluid domain

$$\mathbf{u}_{10} = \mathbf{u}_{20} = 0 \quad (2.3a)$$

and corresponding pressure distributions are given by

$$p_{10} = p_0 + \frac{1}{2}\lambda r^2, \ 0 \le r \le 1 \quad (2.3b)$$

$$p_{20} = p_0 + \frac{1}{2}r^2 - \frac{1-\lambda}{2} - L_2, \ 1 \le r \le \kappa. \quad (2.3c)$$

Consider now arbitary small ($\varepsilon \ll 1$) disturbances to the base flow of the form

$$\begin{bmatrix} u_i \\ v_i \\ w_i \\ p_i \\ \eta \end{bmatrix} = \begin{bmatrix} 0 \\ 0 \\ 0 \\ p_{i0} \\ 0 \end{bmatrix} + \varepsilon \begin{bmatrix} U_i \\ V_i \\ W_i \\ P_i \\ A \end{bmatrix} e^{i(kz+n\theta)+st} \quad (2.4)$$

where U_i, V_i, W_i, and P_i are radial eigenfunctions, A is a constant, k is the axial wavenumber, n is the azimuthal mode number and s is the complex growth rate. In general $s = \sigma + i\omega$, where σ is the real growth rate of disturbances oscillating at frequency ω. It is important to distinguish between different types of disturbance mode described by (2.4). There are planar modes for which $k = 0$; when $n = 0$ the modes are axisymmetric; and when both $k \neq 0$ and $n \neq 0$ the modes are helical. Inserting (2.4) into the full equation of motion (2.1), subtracting the base flow (2.3), and linearizing gives the complex disturbance equations

$$sU_i - 2V_i = -\frac{1}{\lambda^{2-i}} DP_i + \frac{1}{R_i}\left[\left(\mathsf{L} - \left(k^2 + \frac{n^2}{r^2}\right)\right)U_i - \frac{2in}{r^2}V_i\right] \quad (2.5a)$$

$$sV_i + 2U_i = -\frac{in}{r\lambda^{2-i}} P_i + \frac{1}{R_i}\left[\left(\mathsf{L} - \left(k^2 + \frac{n^2}{r^2}\right)\right)V_i + \frac{2in}{r^2}U_i\right] \quad (2.5b)$$

$$sW_i = -\frac{ik}{\lambda^{2-i}} P_i + \frac{1}{R_i}\left[\mathsf{L}_1 - \left(k^2 + \frac{n^2}{r^2}\right)\right]W_i \quad (2.5c)$$

$$\mathsf{D}U_i + \frac{in}{r}V_i + ikW_i = 0. \quad (2.5d)$$

The linearized boundary conditions are

$$P_1 \text{ finite} \quad ,@r = 0 \quad (2.6a)$$

$$U_2 = V_2 = W_2 = 0 \quad ,@r = \kappa \quad (2.6b)$$

$$U_i = sA \quad ,@r = 1 \quad (2.6c)$$

with continuity of normal interfacial stress

$$P_2 - P_1 = \frac{2}{R_2}\left(\frac{\partial U_2}{\partial r} - \chi\frac{\partial U_1}{\partial r}\right) - \Psi A \,,@r = 1 \quad (2.6d)$$

and continuity of the tangential interfacial stress

$$\chi\left[rD\left(\frac{V_1}{r}\right) + \frac{in}{r}U_1\right] = \left[rD\left(\frac{V_2}{r}\right) + \frac{in}{r}U_2\right] \quad ,@r = 1 \quad (2.6e)$$

$$\chi\left[DW_1 + ikU_1\right] = \left[DW_2 + ikU_2\right] \quad ,@r = 1 \quad (2.6f)$$

We have introduced $\Psi = (1-\lambda) + (k^2+n^2-1)L_2$ as the density-dependent generalization of the notation adopted by Boudourides and Davis[1]. The operators L, L_1, D, and D are defined as

$$\mathsf{L} \equiv \mathsf{L}_1 - \frac{1}{r^2}, \mathsf{L}_1 \equiv D^2 + \frac{1}{r}D, \mathsf{D} \equiv D + \frac{1}{r}, D \equiv \frac{d}{dr} \quad (2.7)$$

Note also that interfacial conditions are now evaluated at $r = 1$, the linearized position of the interface.

3. Flow Instability Calculation

Before attempting to solve the boundary value problem, it is useful to search for criteria dictating regions of flow stability. Although the criteria do not give definitive regions for flow instability, they aid in narrowing down the regions in which instability is expected to occur. In the case of an inviscid fluid, stability criteria was derived for axisymmetric, planar, and spiral disturbances by Weidman[9], and the results are summarized in L_2-λ parameter space as shown in Figure 2.

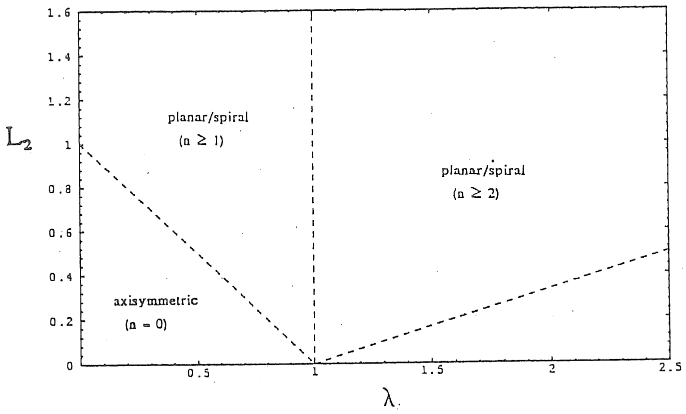

Figure 2 Stability in L_2-λ space. For the modes shown the region of stability is the space enclosed by counter-clockwise rotation of the dashed line about its pivot point at L_2=0, λ=1.

The region of stability for all wavenumbers k of planar/spiral modes for $n \geq 2$ includes the two other regions of stability shown in the sketch; the region for stability of planar/spiral modes for $n \geq 1$ includes the smaller region of axisymmetric stability. The common area which defines stability with respect to all infinitesimal disturbances of modal form (2.4) is the region bounded by the L_2 and λ coordinate axes and the line $L_2 = 1 - \lambda$. Any regions of flow instability must lie outside this triangular region in $L_2 - \lambda$ space.

3.1 Planar Instability

The investigation for inviscid planar disturbances $k = 0$ can be carried out analytically. In this case the axial disturbance velocity $W_i \equiv 0$ in each fluid domain and equation (2.5c)is irrelevant. After some calculation the following eigenvalue relation is obtained[5]

$$(\delta + \lambda)s^2 + 2i(1 - \lambda)s + n\Psi_2 = 0 \quad (3.1a)$$

where

$$\delta = \frac{\kappa^{2n}+1}{\kappa^{2n}-1}, 1 \le \delta \le \infty^5. \quad (3.1b)$$

The eigenvalues are either complex or pure imaginary, the latter determining the sufficient condition for stability. Thus, stability is insured when the discriminant of (3.1 a) is positive, viz.,

$$\left[(\lambda-1)^2 + n(\lambda+\delta)\Psi_2\right] > 0 \quad (3.2a)$$

where

$$\Psi_2 = (1-\lambda) + (n^2-1)L_2 \quad (3.2b)$$

Two ranges of λ are now considered separately. In the range $0 \le \lambda \le 1$ for which the core fluid is lighter than its surrounding annulus, equation (3.2 a) gives

$$(1-\lambda)^2 + n(\lambda+\delta)\left[(1-\lambda) + L_2(n^2-1)\right] > 0 \quad (3.3)$$

keeping in mind that L_2 is always positive, for $n = 1$ inequality (3.3) is satisfied for any value of L_2. When $n \ge 2$ one obtains

$$L_2 > -\frac{\left[n(1-\lambda)(\lambda+\delta) + (1-\lambda)^2\right]}{n(n^2-1)(\lambda+\delta)} \quad (3.4)$$

the right hand side of which is always negative. Hence when $0 \le \lambda \le 1$ the flow is stable to all planar disturbances. Note that $\lambda = 0$ corresponds to a hollow core vortex in solid body rotation bounded by an outer cylinder.

Setting $\Lambda = \lambda^{-1}$, we now consider the range $0 < \Lambda < 1$ for which the outer fluid is lighter than core fluid. Equation (3.2 a) may be written

$$(1-\Lambda)^2 + n(1+\delta\Lambda)\left[L_1(n^2-1) - (1-\Lambda)\right] > 0 . \quad (3.5)$$

The limit $\Lambda \to 0$ corresponding to a cylindrical column of liquid in rigid rotation about its axis warrants special attention since it includes the rotating Rayleigh jet[7] (through a Galilean transformation which does not affect flow stability). In this case (3.5) may be written

$$(n-1)\left[n(n+1)L_1 - 1\right] > 0 \quad (3.6)$$

The lowest planar mode $n = 1$ corresponds to neutral stability; the sufficient condition for stability is given by

$$L_1 > \frac{1}{n(n+1)} \quad n \geqq 2 \quad (3.7)$$

a result originally found by Hocking and Michael[3]. Thus the rotating cylindrical column is stable to all planar disturbances when $L_1 > 1/6$

We note that when (3.7) is not satisfied the flow is unstable and the growth rate of the *nth* unstable planar mode is given by

$$\sigma_m = \sqrt{(n-1)\left[1 - L_1 n(n+1)\right]} \quad n \geqq 2 \quad (3.8)$$

Successively higher modes give rise to higher growth rates, and the transition L_{1t}, found by equating the growth rate of *nth* and (n + 1)*st* modes, is determined to be

$$L_{1t} = \frac{1}{3n(n+1)} \quad n \geqq 2 \quad (3.9)$$

3.2 Instability for the Rotating Liquid Column : $\lambda^{-1}=0$

To our knowledge, the complete inviscid stability boundary for the rotating Rayleigh jet has not been reported. Pedley[6], however, using a small wavenumber approximation to Rayleigh's[7] growth rate equation, demonstrated that n = 3 planar mode was more unstable than n = 0 mode at $L_1 = 0.05$.

The analytical study in 3.1 completes the problem of planar instability for the rotating jet. Numerical results stemming from axisymmetric and spiral disturbances for the single-component rotating jet are presented in this section. We exclude densities in the range $1 < \lambda < \infty$ since the flow is unstable to Rayleigh-Taylor instability for both the planar and axisymmetric modes; moreover, it is difficult to envision how such an initial state for this range of densities might be realized in an actual physical situation.

Axisymmetric Disturbances

The inviscid equation and boundary conditions are given by (2.5) and (2.6) for $i = 1$. Further calculations yield the general eigenvalue relation for the rotating liquid jet

$$\alpha\frac{I_n'(\alpha)}{I_n(\alpha)} = \frac{s^2+4}{1+(1-k^2-n^2)L_1} - \frac{2in}{s}, \quad (3.10)$$

where $I_n(z)$ is the modified Bessel function of the first kind with argument z in general complex, and the prime denotes differentiation of the Bessel function with respect to its argument.

The eigenvalue equation governing axisymmetric disturbances on a rotating jet found by setting $n = 0$ in (3.10) is given by

$$\alpha\frac{I_0'(\alpha)}{I_0(\alpha)} = \frac{s^2+4}{1+(1-k^2)L_1} . \quad (3.11)$$

Maximum growth rates σ_m and the corresponding critical wavenumber k_c are now computed for rotating columns where L_1 is finite. The maximum growth rate is found by first setting $s = \sigma$ in (3.11) and putting differentiation of (3.11) with respect to k equal to zero. One obtains, after some mathematics, the eigenvalue relation

$$\begin{aligned}&(k^2-1)(\sigma^2+4)I_0^{\,2}(\alpha)+2\alpha\sigma^2 I_0(\alpha)I_0'(\alpha)\\&=\left[(k^2-1)(\sigma^2+4)+2k^2\right]I_0'^{\,2}(\alpha)\end{aligned}, \quad (3.12)$$

where $\alpha = \sigma^{-1}\sqrt{\sigma^2+4}$

determining σ_m as a function of k_c [5]. Subsequently, L_1 may be determined from the solution of (3.11) when $k \neq 1$.

Spiral Disturbances

Axisymmetric instability occurs throughout the entire range of wavenumber space and spiral modes exhibit a cut-off wavenumber k_0 [9],

$$k_0 = \sqrt{1-1/L_1}\,. \quad (3.13)$$

For wavenumbers $k<k_0$ both modes of instability are present, and one cannot determine *a priori* which mode will be most unstable. Goto[5] showed that the axisymmetric mode is always more unstable but that σ_m and k_c for the two modes of instability converges as $L_1 \to 0$.

The important results for instability of the rotating Rayleigh jet are summarized in Figure 3 in which growth rate for the first spiral is included for comparison. Axisymmetric instability occurs for all $L_1 > 0.1053$. Below this value the rotating jet is unstable to the $n=2$ planar mode up to the first transition point $L_{1t}=1/18$ at which point $n=3$ planar mode becomes dominant. Successive iterations occur with increasing L_1, apparently *ad infinitum*.

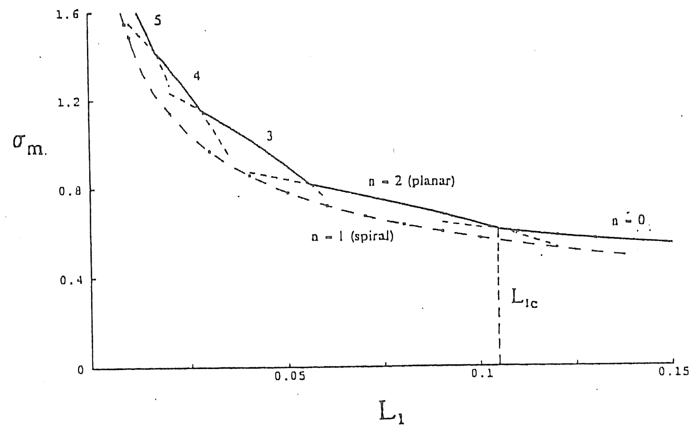

Figure 3 Maximum growth rate for competing axisymmetric, planar, and spiral instability for rotating jet; the solid upper line gives the most unstable mode as a function of L_1.

3.3 Instability for the Two-Fluid System: $0 \le \lambda \le 1$

When the annular fluid is heavier than the core fluid, there is no Rayleigh-Taylor instability and the flow is stable to all planar and spiral disturbances according to the stability criteria results summarized in Figure 2. Here we investigate instability with respect to axisymmetric disturbances.

The equation determining axisymmetric stability and dispersion for the two-fluid system is

$$\begin{aligned}&\left[\alpha\psi_1 I_0'(\alpha)+\lambda(s^2+4)I_0(\alpha)\right]F_1(\alpha,\beta)\\&-(s^2+4)I_0'(\alpha)F_2(\alpha,\beta)=0\end{aligned} \quad (3.14a)$$

where

$$\begin{aligned}F_1(\alpha,\beta) &= I_n'(\alpha)K_n'(\beta)-K_n'(\alpha)I_n'(\beta),\\ F_2(\alpha,\beta) &= I_n(\alpha)K_n'(\beta)-K_n(\alpha)I_n'(\beta)\end{aligned}, \quad (3.14b,c)$$

, $\psi_1 = 1+(k^2-1)L_2$ and $\beta = \kappa\alpha$.
$K_n(z)$ is the modified Bessel function of the second kind with complex argument z.

The Hollow Core Vortex: $\lambda=0$

We first consider the hollow core limit of equation (3.14) obtained by setting $\lambda=0$. Inserting the explicit forms for F_1 and F_2 one obtains the eigenvalue relation. In addition to the liquid jet, Rayleigh[8] considered the stability of a nonrotating hollow core embedded in a fluid of infinite domain for which $\kappa \to \infty$. In this limit the eigenvalue relation reduces to

$$(s^2+4) = \alpha\psi_1\frac{K_0'(\alpha)}{K_0(\alpha)}. \quad (3.15)$$

We now proceed to accurately recompute Rayleigh's[8] critical wavenumber in the nonrotating limit $\Omega \to 0$, remembering that Ω appears in both the nondimensionalization of the complex growth rate and L_2. One obtains the asymptotic relation as

$$s^2 \approx \frac{k(k^2-1)K_0'(k)}{K_0(k)}L_2 \quad (L_2 \to \infty). \quad (3.16)$$

Numerical computation of σ_m and k_c as a function of L_2 at selected value of κ are presented in Figure 4. This figure comprises a summary of results for the rotating hollow core system. Figure 4(a) shows that increasing κ decreases stability; thus for fixed hollow core size, stability is decreased as the volume of surrounding liquid increases. Note also in Figure 4(b) that all critical wavenumbers satisfy $k_c < k_0$ where the cut-off wavenumber is given by[5]

$$k_0 = \sqrt{1 - 1/L_2} \quad (3.17)$$

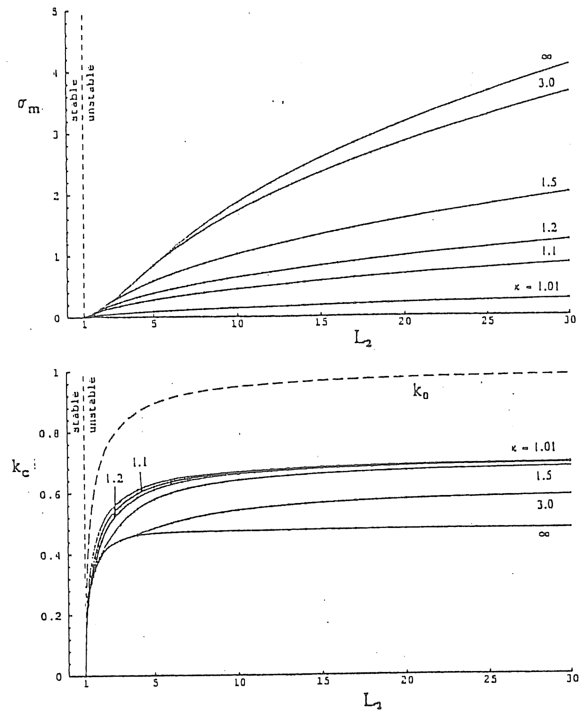

Figure 4 (a) Maximum growth rate and (b) critical wavenumber for axisymmetric instability of the rotating hollow core liquid column at different values of the parameter κ. The dashed line in (b) shows the cut-off wavenumber k_0.

The Two-Fluid System; λ≠0

When both liquids are present, the governing equation for axisymmetric disturbances for arbitary λ, L_2 and κ is given by (3.14). The results of extensive numerical calculations to determine σ_m and k_c over a range of L_2 at λ=0, 1/4, 1/2, 3/4 and 1 for κ=1.2 are plotted in Figure 5. The maximum growth rate curves in Figure 5(a) exhibit a cross-over point at L_{2c}=3.305 where σ_m=0.262. For values L_2<L_{2c}, increasing the density ratio λ yields higher growth rate, an intuitive results for high centripetal acceleration. For L_2>L_{2c}, on the other hand, increasing the density ratio yields lower growth rates. The critical wavenumbers in Figure 5(b) all satisfy $k_c < k_0$ where the cut-off wavenumber k_0 is given by[9]

$$k_0 = \sqrt{1 - (1-\lambda)/L_2} \quad (3.18)$$

Note that each two-fluid system is stable for L_2<1-λ, in agreement with the stability diagram in Figure 2.

4. Conclusion

An investigation of instability of an inviscid, immiscible, two-fluid system in solid rotation has been performed. The system is stable to centrifugal instability

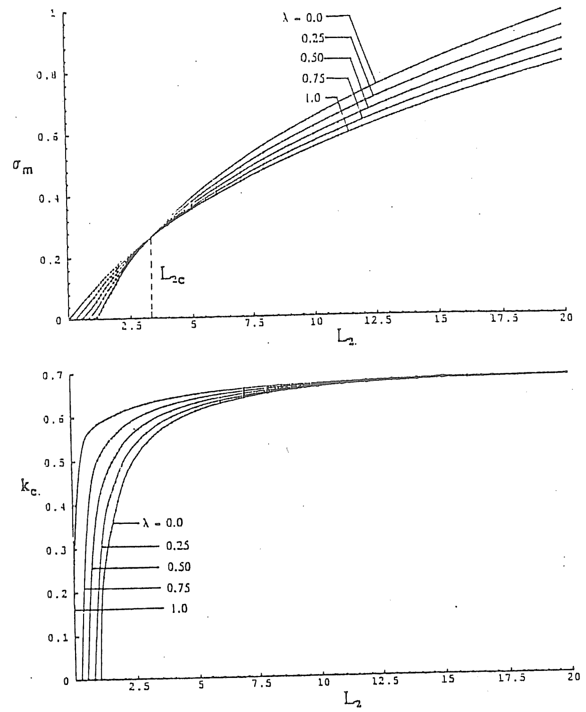

Figure 5 (a) Maximum growth rate and (b) critical wavenumber for axisymmetric instability of the rotating two-fluid column at κ=1.2 for different values of the density ratio λ.

but may undergo Rayleigh-Taylor instability or capillary instability at an interface. An important project for future work would be to carry out a comprehensive viscous stability analysis for this problem.

References

1. Boudourides, M. A. and Davis, S. H. Stability criteria for swirl flows with free surfaces. *J. Appl. Math and Phys.* (ZAMP), **37**, 597-606 (1986).
2. Drazin, P. G. and Reid, W. H. *Hydrodynamic Stability* (Cambridge University Press, Cambridge, 1981).
3. Hocking, L. M. and Michael, D. H. The stability of column of rotating liquid. *Mathematika*, 6, 25-32 (1959).
4. Hocking, L. M. The stability of a rigidly rotating column of liquid. *Mathematika*, 7,1-9 (1960).
5. Goto, M. Instability of rigidly rotating immiscible fluids in zero gravity. University of Colorado Master Theses, (1992).
6. Pedley, T. J. The stability of rotating flows with a cylindrical free surfaces. *J. Fluid Mech.*, **30**, 127-147 (1967).
7. Rayleigh, Lord On the instability of jets. *Proc. London Math. Soc.*, **10**, 4-13 (1879).
8. Rayleigh, Lord On the instability of cylindrical fluid surfaces. *Phili. Mag.*, **34**,177-180 (1892).
9. Weidman, P. Stability Criteria for two immiscible fluids rigidly rotating in zero gravity. *Rev. Roum. Sci. Techn.-Mec. Appl.*, Tome 39, No. 5, 481-496 (1994).
10. Yih, C.-S. Instability of a rotating liquid film with a free surface. Proc. Roy. Soc., 258A, 63-89 (1960)